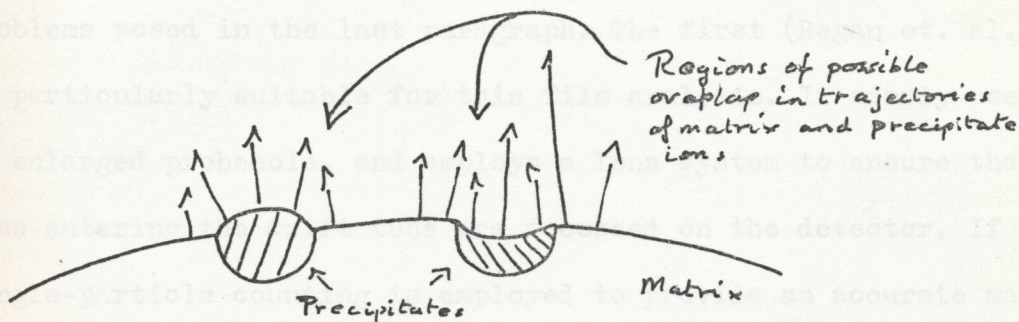


Chapter 5.DESCRIPTION MICROSCOPY AND THE ATOM-PROBE.5.1 Aiming Errors.

Field-desorption microscopy is the imaging of a field-ion specimen surface by the detection of the arrival positions at a microscope screen of field-evaporated metal ions or of desorbed gas ions ; field-evaporation microscopy might perhaps be a better name for the former, self-imaging, process. The work on desorption microscopy described in the following chapters was prompted by a series of discussions on the design and use of atom-probes held in the Cambridge Field-Ion Group; Dr. E.D. Boyes, Dr. M.J. Southon, Dr. P.J. Turner, Mr. A.J. Watts and Mr. D.A. Coppell participated in these discussions and made valuable contributions to them.

As described earlier in this dissertation, the atom-probe FIM is operated by using a probehole in the microscope screen to select a pulse-field-evaporated ion from a particular feature on the specimen surface; the selection is achieved by manipulating the specimen until the field-ion image of the feature lies over the probe-hole. However, it has long been realized (Panitz 1969) that the trajectories of the imaging-gas ions and of the field-evaporated metal ions need not be identical. Attempts have been made to measure differences in trajectories, or 'aiming errors', (Panitz 1969, Brenner and McKinney 1970) by attempting to correlate the disappearance of an atom from the field-ion image with the arrival of an ion at the atom-probe detector. These measurements were necessarily tedious, as very low evaporation rates were essential, and they were restricted to regions of the image where there was good

atomic resolution - thus precluding studies of such important systems as precipitates and solid solutions, where irregular images are frequently observed. Precipitate particles, which commonly have a different evaporation field to the matrix and therefore protrude from or are recessed into the specimen surface, might be expected to have different aiming errors to the bulk, which could lead to spurious analyses:-



Similarly, it is known (e.g. Howell 1972) that there may be a discontinuity in specimen profile when a grain boundary intersects its surface; this could lead to difficulties in the detection of impurity atoms which have been segregated to the boundary, as it is not immediately obvious what trajectories such impurities would follow in the locally-distorted field near the boundary.

Further limitations to conventional atom-probing stem from the use of a small-probehole. This is typically 1-2 mm in diameter in a 50 or 75 mm diameter channel-plate, and subtends an angle of 1 or 2 degrees at the specimen. Analyses performed using such small probeholes are essentially performed on a thin pencil of specimen material; this is useful when a matrix or large precipitates protruding from it, but is less useful when attempting the analysis of thin surface films, thin platelet precipitates, modulations in composition of ordering alloys (Taunt 1973), or grain boundary segregants. In these situations either

an inadequate statistical sample of ions is obtained before the specimen is destroyed, or the detection of a small number of ions is hampered by the lack of certain knowledge about the aiming error associated with these ions.

5.2 Alternative Types of Atom-Probe.

Two possible solutions have been proposed for the problems posed in the last paragraph. The first (Regan et. al. 1972) is particularly suitable for thin film analysis. It simply uses an enlarged probehole, and employs a lens system to ensure that ions entering the drift tube are focussed on the detector. If single-particle counting is employed to provide an accurate mass-spectrum, as in the simple atom-probe, a very low evaporation rate has to be employed to prevent the simultaneous arrival of several ions at the detector: however, the normal field-ion current is now large, with the enlarged probe-hole, and would produce unacceptable noise on the spectrum. This problem was solved by introducing a deflection system to separate the field-ionized gas from the higher-energy pulse-evaporated metal ions. An alternative technique would be to abandon particle counting and digital timing, and to use a large evaporation pulse, so that the mass spectrum would be obtained as an analogue signal from a suitable detector (an electron multiplier or a channel-plate/phosphor/photomultiplier combination). This is largely the approach in the second new type of atom-probe.

This second type of atom-probe (Panitz 1973) attempts to simultaneously mass-analyse ions from a large area of the specimen while preserving crystallographic information on their source position. Ions pulse-evaporated from the specimen are decelerated to 3 KV in

a lens and drift to a detector formed from a curved 'chevron' channel-plate pair, which outputs electrons onto a fast phosphor deposited on a fibre-optic window. A mass spectrum may be obtained from the screen current. Individual atoms may be selected from the normal field-ion picture, after making due allowance for aiming errors, by positioning a light-pipe connected to a photomultiplier at the correct point on the fibre-optic window. Alternatively, a particular mass species may be selected by gating the channel-plate on for a short interval at a preset time after the evaporation pulse, and photographing the scintillations produced on the phosphor.

This last technique would be particularly useful for the study of grain-boundary segregation and perhaps the study of ordering alloys, particularly if the low mass resolution of Panitz's original instrument could be improved. To extract the maximum of information from an analysis it would be necessary to learn the chemical identity and original lattice site of each atom in a sample area of the specimen. However, although this information would be very desirable, it was not clear whether this information could be obtained from a Panitz-type atom-probe. Two immediate difficulties may be seen: first, the limited detection efficiency of the channel-plate assembly, and second, possible 'scrambling' of positional information between the tip and the detected image, as a result of variations in aiming errors. Walko and Muller (1972), who demonstrated the possibility of constructing a desorption microscope using a channel-plate and an external image intensifier to detect the ions, estimated their detection efficiency as about 50%, as limited by the open sensitive area of the channel-plate. They attributed their failure to see regular lattice planes in the desorption image to the random loss of lattice points by the channel-plate.

5.3.1 Objective: Apparatus.

In view of the arguments briefly discussed above, it was decided that a careful study of field-desorption microscopy might lead to useful information on aiming errors, particularly for the complex specimens described above, and would be a useful preliminary to any attempt to use a Panitz-type atom-probe for metallurgical work.

Although Walko and Muller (1972) used a channel-plate and a costly image intensifier, and Panitz used a chevron channel-plate pair to record single ions, it was realized that useful results could be obtained in the first instance by using a single channel-plate at high gain, with fast optics to couple a film to the phosphor screen, as described in Chapter 2 above. A magnetically-focussed channel-plate image-intensifier, which has a higher accelerating potential than the proximity-focussed device used for the energy-analyser, was thought to be desirable, as the electron energy at the phosphor is higher, leading to a brighter image and a slightly higher probability of recording single ions (Turner et al 1969). It was decided to use a UHV field-ion microscope which was fitted with such an intensifier, and which has been described elsewhere (Boyes 1974). The Dallmeyer f 1,9 and Canon f 0,89 lens and camera combination described in Chapter 2 was used to record desorption images on Kodak Tri-X or 2475 film, which were processed as described above. As in the energy-analyser experiments, it was found that 2475 had no significant advantage over the cheaper, but marginally slower, Tri-X, which is well-matched to the P11 phosphor used in the intensifier and which is convenient to handle. Tri-X was used for the majority of the work to be described.

5.3.2 Experimental Technique.

As an ordinary field-ion microscope was used in these experiments, it was possible to compare the normal field-ion image of a surface with a desorption image of the same surface, thereby obtaining a direct measure of aiming errors from all parts of the specimen surface simultaneously. In order to distinguish between field-desorbed ions and field-ionized gas ions, the image gas was pumped out using a mercury diffusion pump before desorbing any material; the evaporation pulse was triggered from the shutter contacts of the camera, at an exposure time of 1/60 second, so that both channel-plate noise and noise from ionized residual gases was minimized. The residual gas pressure, with both inner and outer dewars cooled to 78°K, was typically $1 \cdot 10^{-9}$ Torr or below. Even with a channel-plate voltage of 1500 volts and a screen voltage of 10 KV, very few random ions were recorded on film when the camera shutter was operated without pulsing the specimen voltage.

15 nS, 80 μ S, and 550 μ S pulses were coupled to the tip using a 500 pF coupling capacitor in the usual way, with a high-voltage current-limiting resistor of 1 G Ω between the specimen and a 30 KV Brandenburg H.T. set. Similar results were obtained with each of the pulse lengths, except at very high evaporation rates, as will be discussed below.

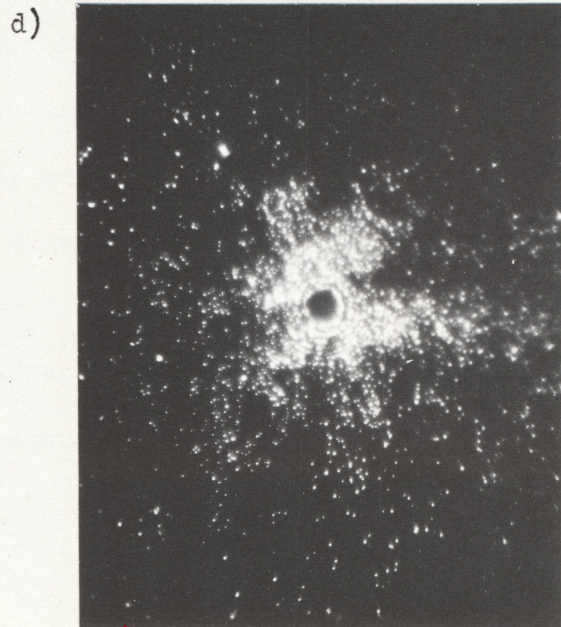
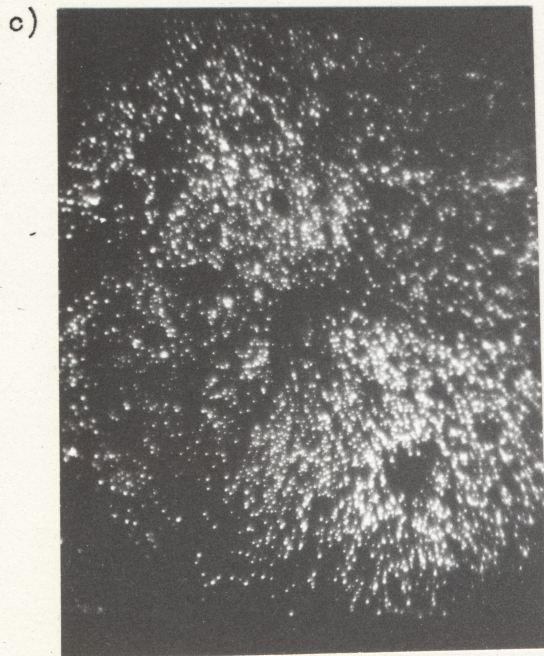
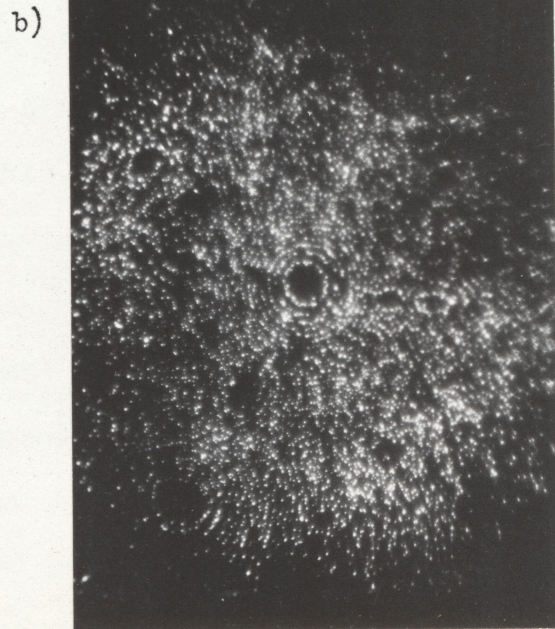
5.3.3 Results.

A tungsten surface which had been exposed to helium image gas was found to produce pulse-evaporated ions at a slightly lower field than was necessary for subsequent vacuum field-evaporation. Comparison of helium images of the surface before and after pulse-evaporation in vacuo showed that tungsten atoms were

Fig. 5.1

Tungsten pulsed-field desorption micrographs, 78°K.

- a) Helium image of specimen b) Typical desorption micrograph showing
110 ring structure c) 200 -type image after exposure to helium
d) Atypical irregular image, due to a change in specimen profile.



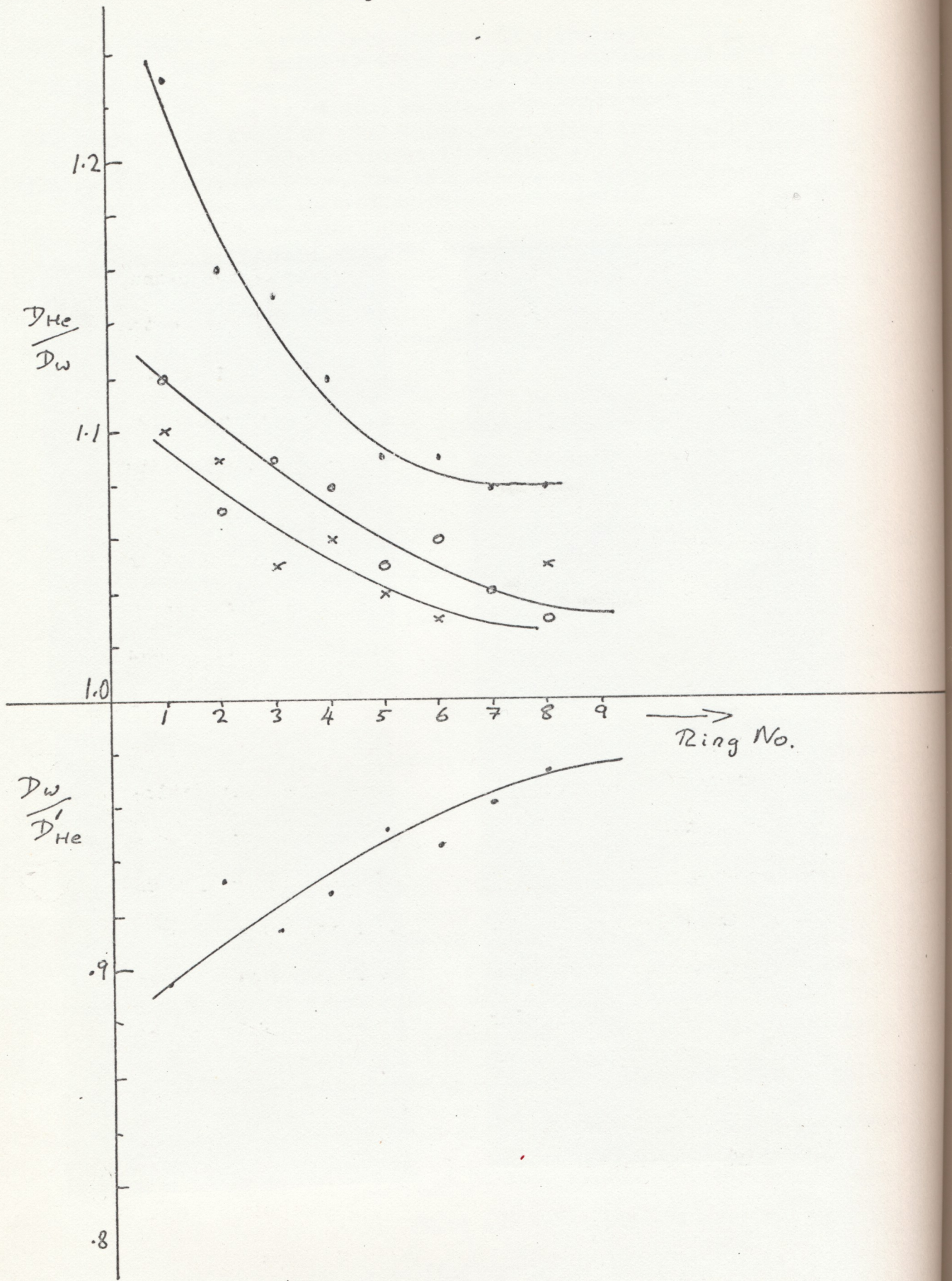
removed from the surface as well as field-adsorbed helium, as was expected from atom-probe results (Muller et al 1969). The evaporation field was lowered by approximately 5% by exposure to helium before evaporation in vacuum. The image-points produced by desorbed helium ions and tungsten ions could not, of course, be distinguished in this experiment.

Some typical desorption images are shown in fig(5.1), with a helium image for comparison. A system of rings centred on $\{110\}$ planes was the most commonly observed type of pattern, especially after repeated evaporation in vacuum (fig(5.1b)). Square patterns centred on $\{200\}$ planes could be obtained when the specimen had been exposed to helium; there is presumably a slight change of specimen endform when this type of pattern is produced. Occasionally, particularly at low evaporation rates or in poor vacua, evaporation occurred irregularly across the surface, producing an intermediate type of desorption image (fig(5.1d)). Similar patterns to those in fig(5.1b and c) have been reported by Walko and Muller (1972) and Panitz (1973).

5.3.4 Measurement of Aiming Errors for Tungsten.

Aiming errors for the $\{110\}$ ring-type desorption could be simply measured (for the radial direction) by measuring the diameter of each helium image ring before desorption, and comparing it with the diameter of the corresponding ring in the tungsten desorption image. A plot of $d_{\text{He}}/d_{\text{des}}$ versus ring number, counting out from the centre of the (110) plane, was made for three different zones and is shown in fig(5.2). The diameter of the relatively thick helium image rings which was taken was the mean diameter. Care was taken to ensure that no changes in magnification

Fig. 5.2



UNIVERSITY OF CAMBRIDGE

of the images had occurred, due to the change in tip potential during the pulse, as a result of the low negative potential which is applied to the front of the channel-plate in the design of intensifier which was used. It was found that the {222} planes in the helium and desorption images coincided to within the limits of measurement. As can be seen from the graph, the aiming error varies with distance from the centre of the plane, and may be as large as 25 % of the ring diameter for the central ring. The diameters of the rings in the desorption image were less than those of the corresponding rings in the helium image. This agrees with Brenner and McKinney's conclusions (1970); they found that they detected tungsten ions when they positioned the probe-hole of their atom-probe slightly on the inside of the helium image of a {110} ring. A plot of $d_{\text{He}}^i/d_{\text{des.}}$, where the superscript indicates the helium ring after the desorption, was also made, and is shown in the figure. It is seen that the ratio is still greater than unity; this illustrates the fact that the desorption image cannot be simply regarded as a tungsten field-ion image of the surface remaining after evaporation, as might be supposed. It should perhaps be emphasized that a 25 % aiming error for the central ring is in fact quite a small effect; the diameter of the ring was only some 40-60 Å, so the atom-probe probe-hole would only need to be aimed some 5-8 Å closer to the centre of the plane to catch the ions from the ring.

5.3.5 Detection Efficiency.

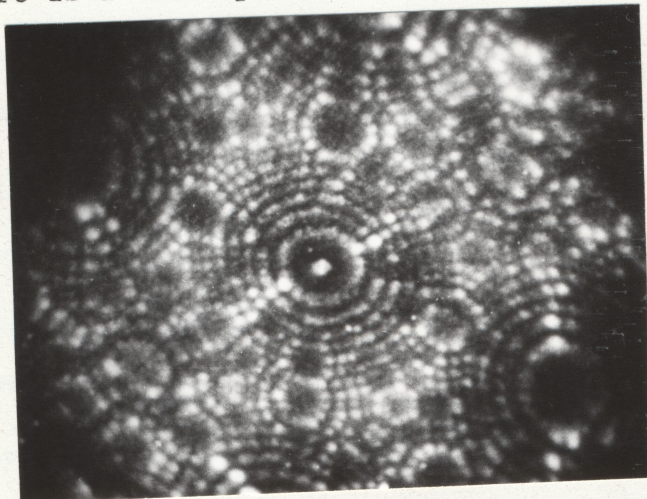
Measurement of aiming errors in the relatively flat {110} region of tungsten was fairly easy, as many ions were available, forming clearly-distinguished rings. However, as originally pointed out by Brenner and McKinney (1970), when the local curvature

DEPARTMENT OF METALLURGY

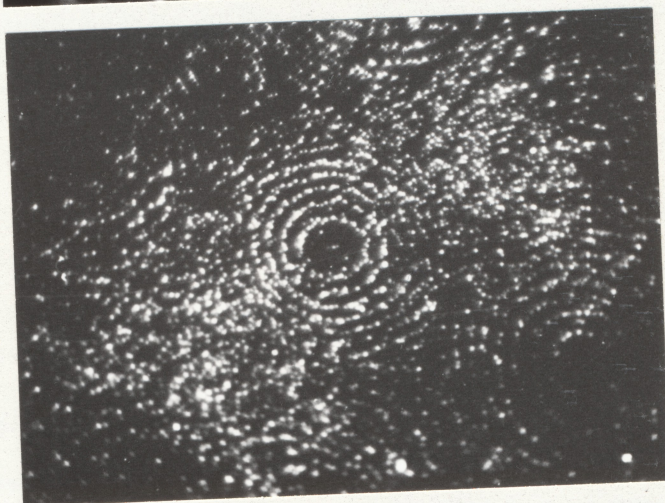
Fig. 5.3

Sequence of pictures illustrating the successful detection of a cluster of atoms desorbed from (110). a) Helium image of tungsten specimen, showing cluster b) Desorption image c) Helium image after desorption. There is a 'lit-up' channel inside the central 110 ring.

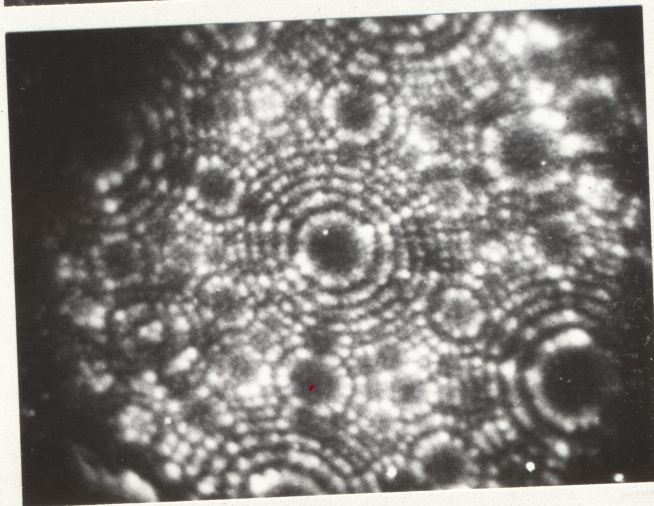
a)



b)



c)



of the surface is high, as for the $\{222\}$ planes in tungsten, the evaporation of a complete plane is expected to produce only a few well-separated ions on the desorption image, as the plane is small and highly-magnified. This effect was observed, and limited attempts to determine the detection efficiency by evaporating a $\{222\}$ plane and attempting to correlate the removal of the well-resolved atoms from the plane with the arrival of ions in the corresponding region of the desorption image. The situation was further complicated by the impossibility of discriminating between field-adsorbed helium and tungsten atoms. Attempts to superpose consecutive vacuum desorption images failed to produce any satisfactory evidence for the aiming-errors associated with $\{222\}$ planes or for the overall detection efficiency of the system. Two modifications to the experiment were therefore tried.

In the first, the specimen was evaporated until only a small cluster of atoms remained at the centre of the central (110) plane. The image gas was removed, and a small evaporation pulse applied. The image gas was then readmitted, to see whether the cluster had been removed or not. An example of the results is shown in fig(5.3). In this example ions were detected in the desorption image close to the position of the original cluster; frequently this was not the case, and either no ions attributable to the cluster were detected, or they were displaced from the centre of the plane. There seemed to be a better chance of detecting the ions close to the helium image of the cluster if a relatively large evaporation pulse was used. This seems to suggest that at intermediate pulse-heights there is a possibility of the cluster migrating some distance across the plane before desorbing, and that this effect, in combination with the less-than-100 % detection efficiency,

was responsible for the frequent failure to detect ions from the cluster in the expected central position in the image. This result was not entirely unexpected, as Turner (private communication) had observed that positioning the atom-probe probe-hole directly over the centre of the tungsten (110) plane leads to a particularly low ion catch-rate. Boyes (1974) had also observed that in gold specimens the last few atoms to evaporate from a $\{200\}$ plane frequently migrate considerable distances before desorbing; this was observed under neon imaging conditions at 20°K. Therefore the failure to detect the evaporated clusters conclusively may be due to

- 1) genuinely low detection efficiency
- 2) diffusion of the cluster before evaporation
- 3) evaporation of the cluster from the centre of the plane,

but subsequent deflection, as by coulomb repulsion between atoms evaporating simultaneously.

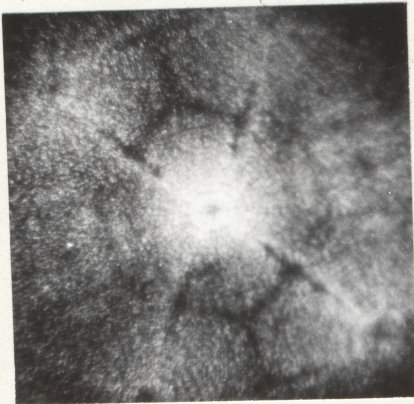
Evidence that one of the latter two reasons is the correct one will be presented below.

The second attempt to determine detection efficiency was made by attempting to evaporate a complete $\{222\}$ plane in a single pulse, to see if the net plane structure could be resolved. When this was done, by using a large evaporation pulse, two things became apparent. First, it was still difficult to correlate the few desorbed ions detected in the $\{222\}$ regions with the corresponding atoms in the helium image. Second, and more important, was the fact that when large quantities of material (1 or more central $\{110\}$ planes) were removed per pulse, the intensity distribution in the desorption image was not simply a slowly-varying gradation, with density inversely proportional to the local magnification, as might be expected. Instead, a marked pattern of dark lines began to be apparent.

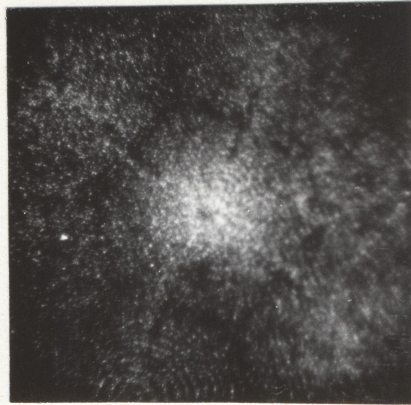
Fig. 5.4

A sequence of tungsten desorption micrographs with progressively less of the specimen being evaporated to form the image.

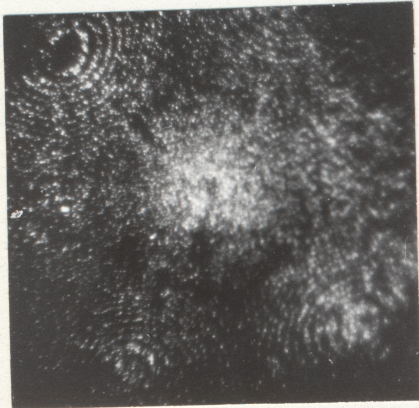
1)



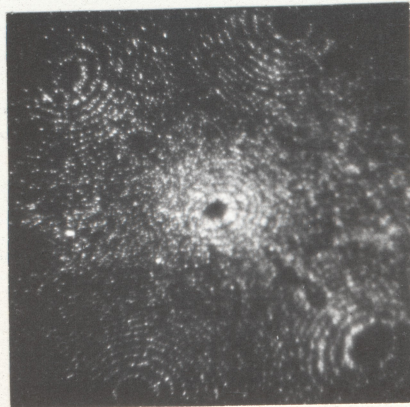
2)



3)



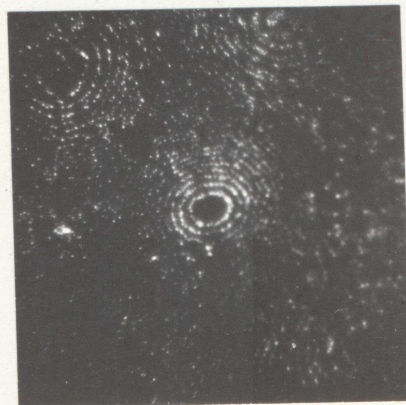
4)



5)



6)



Raising the size of the evaporation pulse, to increase the thickness of the shell of material removed from the specimen, simply accentuated the dark lines, rather than removing them. A sequence of desorption images (fig(5.4)) taken with a fixed pulse height and standing voltage, in UHV, illustrate that the structure which is clearly seen in the high-coverage pictures is not evident in the low-coverage pictures merely because of the lack of sufficient image points to delineate it. This result was confirmed by a method which will be described below. It will also be confirmed that the structure in the desorption image is not due simply to a change in the profile of the specimen, due to changing evaporation rate or other effects. The structure in the desorption image may be obtained on many consecutive pulses, if the number of ions in the desorption image is maintained by increasing the standing voltage or using a suitably finely-tapered specimen.

Comparable structured high-coverage desorption images were obtained from aluminium and molybdenum at this stage (these will be presented in Chapter 6). It was found that the high brightness of the magnetic image-converter is offset by a disadvantage in this type of experiment. It was found that the brightest regions of the desorption images were poorly-focussed; this was a defect of the converter, and not of the external optical system. The effect was attributed to space-charge defocussing in the 70 mm gap between the channel-plate and the phosphor screen. At a high evaporation rate, approximately 10^3 ions may arrive per cm^2 of the channel-plate in 15 nS: assuming a gain of 10^4 , the electron current density at the output of the plate will be about 10 A/m^2 . According to Child's Law (Bleaney and Bleaney 1967) the limiting current density J in a plane parallel diode is given by

$$J = \frac{4}{9} V^{3/2} \epsilon_0 d^{-2} (2 e/m)^{1/2}$$

$\approx 850 \text{ A m}^{-2}$ for the dimensions and voltages of the present converter. The current density in the converter is sufficiently near to the absolute maximum for defocussing by space-charge effects to be a real problem (this will also apply, of course, to an image intensifier external to the system (e.g. Walko and Muller 1972)). Dr. A.J. Moore and Dr. J. Spink repeated the experiment, using a tungsten specimen and a proximity-focussed channel-plate intensifier, which has a short electron path in a high electric field, and this did not suffer from any defocussing even at very high current levels. The remainder of the work on field desorption, with a few exceptions, was therefore done using proximity-focussed intensifiers.

5.4 Summary.

The results obtained at this stage showed that desorption microscopy could provide useful information on aiming-errors in the atom-probe, which are of interest in view of the widening application of atom-probing to complex specimens of metallurgical interest. Brenner and McKinney's original conclusions on the direction of aiming errors in the $\{110\}$ region of tungsten were found to be reasonable, although, as will be explained in Chapter 8 their explanation of the effect in terms of parallax is not accepted. Attempts to determine the detection efficiency of the recording system were not entirely successful, and the discovery of a marked and unexpected structure in the desorption images from tungsten, aluminium, and molybdenum suggested that the apparently low detection efficiency might perhaps have a common origin with the phenomenon of aiming errors itself. The detection efficiency

of the of the microscope was difficult to measure with any certainty, but in the light of present knowledge and by comparison with the results presented by Walko (1972) and Panitz(1973) the detection efficiency probably lay in the range 30-50%.

It was decided that, in the light of these results, a further study of desorption imaging was vital to the sensible use of the atom-probe in metallurgical systems, and, in view of the unexpected structure in the desorption image, would probably provide useful information on the mechanisms involved in field-evaporation. A considerable amount of work was then undertaken, and this will be reported in Chapters 6 and 7 below.

The experimental technique used in the last chapter, pulse evaporation, and detection of the desorption image with a high-gain magnetic converter and fast optics, was not considered desirable for the following reasons. Firstly, the magnetic converter was known to suffer from defocussing at high intensities, so a proximity-focussed converter was required. Secondly, to obtain a complete high-coverage desorption pattern from one evaporation pulse required a very high evaporation rate: to evaporate ten planes in ten nanoseconds implies an evaporation rate of 10^9 planes/second. Although such rates can be achieved with robust specimens, the field-stress is so high that tip failure is a frequent event. The alternative technique, that of superimposing on one negative the desorption patterns from consecutive low-rate pulsed evaporations, was not possible at the time as a suitable evaporation pulser